ESR study of the hydrogen-potassium-graphite ternary intercalation compounds

Toshiaki Enoki* and Hiroo Inokuchi
Institute for Molecular Science, Okazaki 444, Japan

Mizuka Sano
Department of Chemistry, Faculty of Science, Kumamoto University, Kumamoto 860, Japan
(Received 27 January 1987; revised manuscript received 7 July 1987)

The electronic properties of the stage-1 and -2 hydrogen-potassium-graphite ternary intercalation compounds (KH-GIC's) $C_{4n}KH_x$ ($n=1,2$; $x\sim0.8$) were investigated by means of ESR measurements. The observed temperature dependence of the diffusion time is found to be associated not only with the conduction-electron spins but also with the localized spins. The behavior of the paramagnetic susceptibilities and the g values gives additional evidence for the presence of localized spins which interact with the conduction-electron spins. The KH-GIC's possess the ionic lattice of the donor intercalant with sandwich layers K^+-H^--K^+, which are affected by the conduction electrons on the graphite layers. The composition $C_{4n}KH_{0.8}$ suggests hydrogen deficiency in the K^+-H^--K^+ ionic intercalant, which gives defects in the intercalant. The presence of the localized spins is attributed to trapped electrons at the defects in the intercalants. The spin relaxation at high temperatures is explained with use of the Elliott mechanism. The exchange interactions between graphite π and alkali-metal s electrons and the large spin-orbit interaction of alkali-metal atoms play important roles in the relaxation process.

I. INTRODUCTION

C_8K acts as a catalyst in some hydrogen reactions: the H–D exchange reaction and ortho–parahydrogen conversion.[1] Hydrogen absorption, based on the catalytic activities of C_8K at room temperature, produces the hydride C_8KH_x, in which, for low hydrogen concentrations $x\lesssim0.1$, hydrogen atoms dissociated through a chemisorption process sit at interstitial sites among the K atoms in the intercalant layers. Further hydrogen uptake brings about a structural change to a second-stage structure with sandwiched intercalants including double K layers between which an H layer is inserted. The second-stage structure is completed at a saturated hydrogen concentration $x\sim0.67$.[2,3] The hydride $C_{4n}KH_x$ (stage number $n=1,2,3,\ldots$), where the hydride with $n=2$ has the same structure as that obtained by the hydrogen chemisorption described above, can also be prepared by the direct intercalation of the ionic hydride KH into graphite.[4] In this case, the hydrogen concentration can reach $x\sim0.8$, which is larger than the saturated concentration for the chemisorption process. The alkali-metal–hydrogen ternary graphite intercalation compounds are known to be isostructural to the alkali-metal–mercury ternary graphite intercalation compounds, $C_{4n}KHg_x$.[4,5]

The hydrogen deficiency ($x\sim0.67$–0.8) in the intercalant lattice K^+-H^- plays an essential role in providing an opportunity to bring about a charge transfer from the intercalant to graphite layers, leading to the formation of the graphite intercalation compounds. The deficiency is also an important feature in the relation between the structure and the electronic properties.

In the potassium-hydrogen ternary graphite intercalation compounds, the electronic properties investigated by means of the specific-heat[6] and the Shubnikov–de Haas effect,[7] are found to be characteristic of an ionic donor intercalant K^+-H^- inserted between a metallic medium of graphitic layers where most of the electron carriers exits. On the other hand, conductivity (Ref. 8) and H-NMR (Ref. 9) measurements suggest the presence of a small number of carriers on the hydrogen atoms in spite of the ionic system. Among the many kinds of metal hydrides, transition-metal hydrides such as PdH_x are regarded as metallic alloys between the transition metal and hydrogen, where the hydrogen species possesses delocalized electronic states associated with the large screening effect of the conduction electrons from the metal atoms. At the other extreme, the electronic state of hydrogen in alkali-metal hydrides such as K^+-H^- is described in terms of a hydride anion H^- with localized character, since these hydrides are ionic insulators. Among the metal hydrides, ternary graphite–alkali-metal hydrides are special; the presence of a small number of charge carriers on the hydrogen atoms will produce novel electronic properties, though the overall features of the intercalants K^+-H^- seem to be ionic with localized character.

The present paper concerns an ESR experiment in ternary graphite potassium hydrides, $C_{4n}KH_x$ ($n=1,2$). Up to now, many ESR experiments have been carried out in graphite intercalation compounds (GIC's) where the ESR signals show the Dysonian shapes of conduction-electron spin resonance because of the metallic properties of GIC's.[10–16] Recently, Blinowski *et al.*[17] and Saint Jean *et al.*[18] pointed out the necessity for consideration of the geometry of the samples in the measurement of conduction-electron spin resonance for graphite inter-

calation compounds which have two-dimensional anisotropic conductivity. We take into account the geometrical dependence of the line shape in our experiment. The present paper also contains a discussion of the relation between the experimental results of ESR and the transport phenomena, in connection with the structural problem in $C_{4n}KH_x$ compounds.

II. EXPERIMENT

Samples of stage-1 and -2 hydrogen-potassium-graphite ternary intercalation compounds $C_{4n}KH_x$ ($n=1,2$) (KH-GIC's) were prepared by a direct intercalation method. Highly-oriented pyrolytic graphite [(HOPG), Union Carbide UCAR] and KH powder sealed in a vacuum Pyrex tube were treated in a furnace for about two weeks at 430 °C and 250 °C for stage-1 and -2 KH-GIC's, respectively. The as-prepared samples were characterized by (001) x-ray diffraction, and transferred to quartz ESR tubes in an Ar glove box operated at an impurity level of 1 ppm. The sample was mounted on a Teflon holder in an ESR tube where 20-Torr He gas was sealed as a heat exchanger. ESR spectra were measured using a conventional X-band spectrometer (Varian E112) with a rectangular TE_{102} microwave cavity and a continuous-flow He cryostat (Oxford ESR-9) between liquid-helium and room temperatures. To investigate the dependence of ESR line shapes on the shapes of samples, three kinds of sample dimensions were employed (see Fig. 2): $l\times w\times d$=(1) $3\times2.5\times0.25$ mm^3, (2) $5\times0.5\times0.25$ mm^3, and (3) $2\times2\times0.25$ mm^3, where the c axis of the sample was parallel to the d direction, an oscillating magnetic field H_1 was applied in parallel to the l direction for cases (1) and (2), and d for case (3), respectively. A static field H was applied perpendicular to the l direction for cases (1) and (2), and d for case (3), respectively.

As exhibited in Fig. 1, ESR spectra showed asymmetric Dysonian line shapes for stage-1 and -2 KH-GIC's which suggest the metallic nature of the materials. The sample dependence of the shape was small enough to investigate the characteristic features of these materials if the samples were in the same geometrical arrangement. The microwave-power dependence and modulation-frequency dependence of the ESR spectra were taken in the power range between 10^{-2} and 10^2 mW and in the frequency range between 35 Hz and 100 kHz, respectively. The intensity of ESR spectra was found to be a linear function of a square root of power up to 10^2 mW (maximum power available in our instrument) even at liquid-helium temperature. This means the absence of the saturation effect in the present experiment. The line shape including the asymmetry parameter A/B [the ratio of the heights between the maximum (A) and the minimum (B) of ESR spectra] for the Dysonian line shape was revealed to be independent not only of the microwave power, but also of the modulation frequency, in disagreement with the experimental results for C_8AsF_5 which suggested the inapplicability of the Feher-Kip procedure[19] for the line-shape analysis of the Dysonian signal in anisotropic conductors such as acceptor compounds with large in-plane to c-axis conductivity ratio σ_a/σ_c.[18] The asymmetry pa-

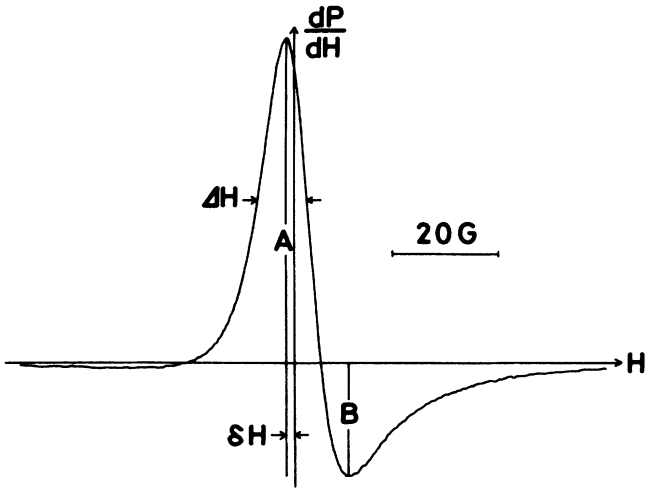

FIG. 1. The first derivative of an ESR spectrum of the stage-1 KH-GIC at 289 K under applied field perpendicular to the c axis. A and B denote the heights of the maximum and the minimum of the spectrum, respectively. δH denotes the deviation of the maximum peak from the resonance center of the spectrum; Δ is the linewidth. The geometrical arrangement of the sample belongs to case (1) (see text).

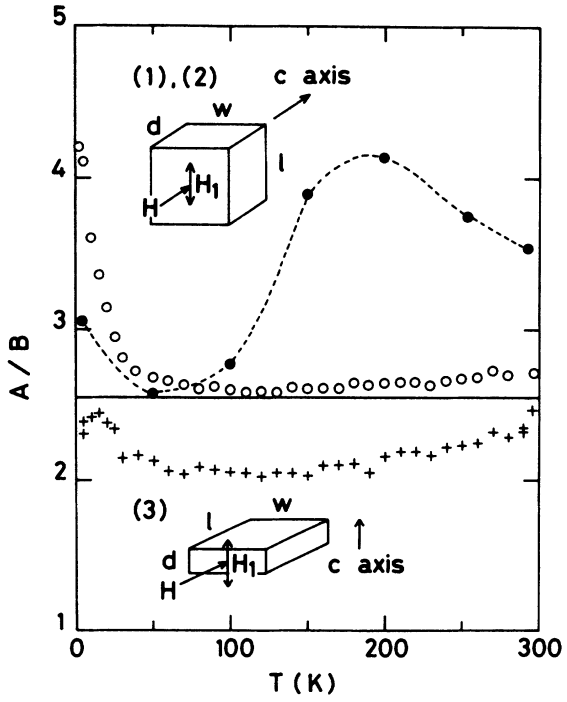

FIG. 2. Geometrical dependence of the asymmetry parameter A/B. The samples have the dimensions (1) $l\times w\times d$ $=3\times2.5\times0.25$ mm^3 (○), (2) $5\times0.5\times0.25$ mm^3 (●), and (3) $2\times2\times0.25$ mm^3 (×). The d direction is parallel to the c axis. The static field H is applied perpendicular to the l direction for (1) and (2), and the d direction for (3), respectively. An oscillating field H_1 is applied in parallel to the l direction for (1) and (2), and parallel to d for (3), respectively. The solid line gives the slow diffusion limit.

rameter A/B was found to depend on the geometry of the sample as shown in Fig. 2 for the stage-1 KH-GIC. In the case of the sample with the dimension of $1\times w\times d=2\times 2\times 0.25$ mm^3, the applied field parallel to the l direction and the microwave field parallel to the c axis (parallel to the d direction), A/B possesses the observed value below the slow-diffusion limit 2.55 (infinite diffusion time $T_D\rightarrow\infty$) with a weak temperature dependence. The reason for the small A/B is that the observed spins in the experiment exist in the boundary regions just beneath the surfaces of the sample where the motion of the conduction carriers is disturbed by a large irregularity in the crystal lattice since the microwave skin depth, $\delta=c(2\pi\omega\sigma_a)^{-1}$, related to good in-plane conduction σ_a^8 is quite shallow and the microwave propagates in parallel to the c plane. For cases (1) and (2), the samples are exposed to microwave radiation at two sides. One side is perpendicular to the c axis where the microwaves propagate in parallel to the c axis in the surface region within the shallow skin depth $\delta_c=c(2\pi\omega\sigma_a)^{-1/2}$ related to the large magnitude of σ_a, while the other side is parallel to the c axis with the deep skin depth of $\delta_a=c(2\pi\omega\sigma_c)^{-1/2}$ given by the small magnitude of c-axis conductivity σ_c^8. The ratio of the observed regions between the two sides is described by $\gamma=lw\delta_c/1d\delta_a$. From the conductivity measurement for C_4KH_x ($\sigma_a=2.1\times10^4$ $\Omega\,\mathrm{cm}^{-1}$ and 6.9×10^5 $\Omega\,\mathrm{cm}^{-1}$ at 300 and 4.2 K, $\sigma_c=5.9$ $\Omega\,\mathrm{cm}^{-1}$ and 64 $\Omega\,\mathrm{cm}^{-1}$ at 300 and 4.2 K, respectively),[8] the skin depths are estimated at $\delta_c=3.6\times10^{-4}$ cm and 6.4×10^{-5} cm at 300 and 4.2 K, and $\delta_a=0.022$ cm and 6.6×10^{-3} cm at 300 and 4.2 K, respectively, for X-band microwaves with 9.1 GHz. The skin depths give estimates of the ratios γ; 0.16 and 0.10 at 300 and 4.2 K, respectively, for case (1), and 0.03 and 0.02 at 300 and 4.2 K, respectively, for case (2). The magnitudes of γ suggest that the observed spins in the ESR experiments are associated mainly with the surface region parallel to the c axis. The difference in the parameter A/B between cases (1) and (2) is ascribed to the geometrical difference of the samples which modifies the contribution from the surface region perpendicular to the c axis. Thus, the geometrical differences of the two-dimensional conductors make quantitative analysis difficult, so that the observed line shapes in the KH-GIC systems are understood only qualitatively by means of the Feher-Kip procedure for the one-dimensional line-shape analysis of Dysonian signals with a skin depth of δ_a and an in-plane conductivity of σ_a,[17,18] where microwave radiation works for the ESR detection of electrons existing around the surface region parallel to the c axis. Here, we have to be satisfied with rather qualitative explanation of the ESR results, though the future development of theoretical works will offer a clue to make quantitative analysis for the detailed experimental results.

III. RESULTS AND DISCUSSION

We calculate the g values, the spin-relaxation time T_2, and the diffusion time T_D, using the Feher-Kip equation[19] for the samples described in case (1). In this procedure, the problem of electron diffusion is treated in connection with the paramagnetic resonance in metals, and the following expression is given for an ESR spectrum:

$$I=-\left[\frac{\omega H_1^2}{4}(\delta A)\omega_0\chi T_2\right]\frac{T_D}{2T_2}\left[\frac{R^4(x^2-1)+1-2R^2x}{[(R^2x-1)^2+R^4]^2}\left[\frac{2\xi}{R(1+x^2)^{1/2}}+R^2(x+1)-3\right]+\frac{2R^2-2xR^4}{[(R^2x-1)^2+R^4]^2}\left[\frac{2\eta}{R(1+x^2)^{1/2}}+R^2(x-1)-3\right]\right], \tag{1}$$

where $x=(\omega-\omega_0)T_2$, $\xi=\mathrm{sgn}x[(1+x^2)^{1/2}-1]^{1/2}$, $\eta=[(1+x^2)^{1/2}+1]^{1/2}$, $R=(T_D/T_2)^{1/2}$, δ is the skin depth, A the area of surface, χ the paramagnetic part of the static susceptibility, and ω_0 is the resonant frequency satisfying the condition $\hbar\omega_0=g\beta H$. The first derivative of Eq. (1) with x shows an asymmetric line shape with an asymmetry parameter A/B, as illustrated in Fig. 1. The g value, T_D, and T_2 can be calculated using A/B; the linewidth ΔH and the deviation of the maximum peak from the resonant field δH, using the numerical calculation of Eq. (1). The g values are summarized in Table I for the stage-1 and -2 KH-GIC's with the applied fields parallel and perpendicular to the c axis. The magnitudes of the g values $g_\parallel$ and $g_\perp$ are close to the g value of the free-electron spin. The anisotropies in the g values, $g_\parallel-g_\perp$ are 6×10^{-4} and 5×10^{-4} for the stage-1 and -2 KH-GIC's, respectively, which are considerably smaller than the anisotropy in pristine graphite and possess an opposite sign from that of pristine graphite. The situation is quite similar to that of the K-GIC's.

The asymmetry parameters A/B are presented in Fig. 3 for the stage-1 and -2 KH-GIC's. In the case of the stage-1 compound, A/B decreases weakly as the temperature is lowered, and then, below about 50 K, it increases steeply. As for the stage-2 compound, A/B depends on

TABLE I. g values of $C_{4n}KH_x$.

	$g_\parallel$	$g_\perp$
C_4KH_x	2.0031	2.0025
C_8KH_x	2.0018	2.0013

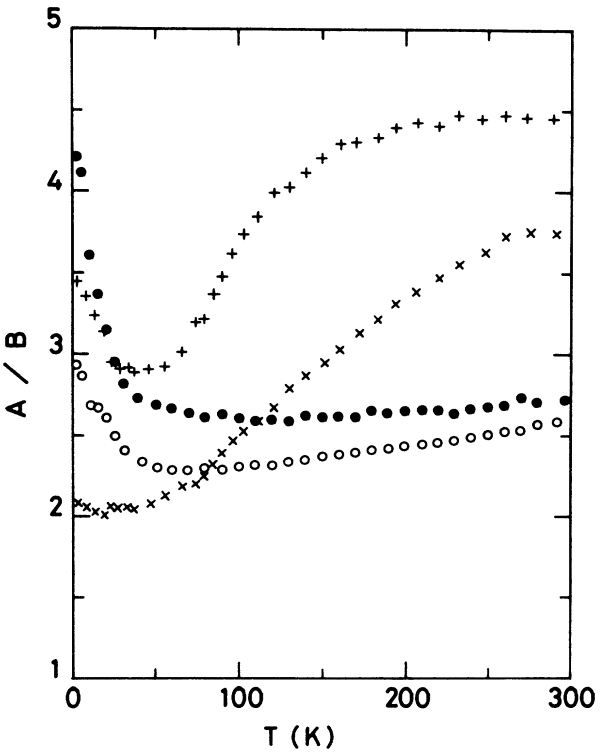

FIG. 3. Temperature dependence of the asymmetry parameter A/B. The stage-1 KH-GIC: ●, H⊥c; ○, H∥c. The stage-2 KH-GIC: ×, H⊥c; +, H∥c.

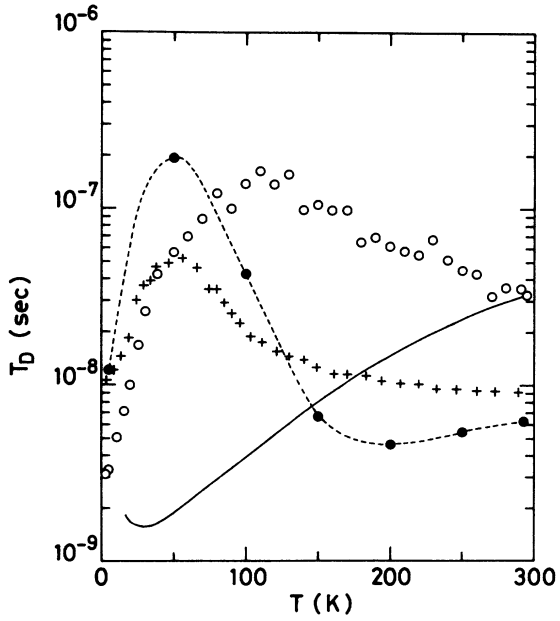

FIG. 4. Temperature dependences of the diffusion time T_D. The open and solid circles denote the results for the stage-1 samples with the dimensions (1) $l\times w\times d=3\times 2.5\times 0.25$ mm^3 and (2) $5\times 0.5\times 0.25$ mm^3, respectively. The crosses denote the results for the stage-2 sample with the dimension $l\times w\times d=3\times 2.5\times 0.25$ mm^3. The field is applied perpendicular to the c axis. The solid line denotes the diffusion time estimated from the conductivity measurement where the value at $T=295$ K is reduced to the value calculated from the ESR measurement.

the direction of the applied field more strongly than that for the stage-1 compound. A/B decreases weakly at high temperatures above 150–200 K on lowering the temperature. Below these temperatures, it decreases steeply and then, below about 50 K, it shows an increase. The Feher-Kip procedure gives the diffusion time T_D of the carriers within the skin depth, as shown in Fig. 4. For the stage-1 sample with the dimension of $l\times w\times d=3\times 2.5\times 0.25$ mm^3, T_D increases as the temperature is lowered while it decreases steeply below 100 K. For comparison, we present the results with different dimensions. The sample with a dimension of $l\times w\times d=5\times 0.5\times 0.25$ mm^3 shows an additional temperature dependence at high temperatures where T_D decreases weakly with lowering temperature. The maximum of T_D is shifted to the low-temperature side, in comparison with the results of the sample with $l\times w\times d=3\times 2.5\times 0.25$ mm^3. As mentioned in the preceding section, the samples are exposed to microwave radiation on two sides. The mixing ratio of the observed surface regions between the two sides is different for the different sample shapes. Thus, the difference in the behavior of T_D is considered to be associated with the difference in the magnitude of the ratio for the different samples. For the stage-2 compound, T_D shows a maximum around 50 K, below which the decrease in T_D becomes steep.

The diffusion time can also be estimated by means of conductivity measurements.[8] The diffusion time parallel to the a axis is given by the equation

$$T_D^a=\frac{\delta_a^2}{2D_a}\ , \tag{2}$$

where D_a is the diffusion constant parallel to the a axis which is described by the Einstein relation for the mobility μ_a, $D_a=\mu_a kT/e$. Therefore, we can estimate the diffusion time from the conductivities σ_a and σ_c in the following way:

$$T_D^a=\frac{ne^2c^2}{4\pi\omega}\frac{1}{kT\sigma_a\sigma_c}\ , \tag{3}$$

where n is the carrier density. The derivation of Eq. (2) shown above suggests an equivalency between T_D^a and T_D^c. The diffusion time T_D^a of the stage-1 KH-GIC estimated by Eq. (3) with the conductivity measurement is also shown in Fig. 4, for comparison. The diffusion time decreases monotonically when lowering the temperature down to about 20 K, and then it increases below 20 K. The behavior of the diffusion time is different from that of the diffusion time derived from the ESR measurement. The experimental fact that T_D derived from ESR is considerably larger than that from the conductivity measurement suggests that, for the former T_D, the contribution to T_D is associated not only with the conduction-electron spins, but also with the localized spins with an infinite diffusion time which work to make the observed diffusion time effectively large at low temperatures because of the

increase in the susceptibility of the localized spins on the lowering temperature.

The temperature dependences of the spin paramagnetic susceptibility χ and the g value are shown in Fig. 5 for the stage-1 KH-GIC. The magnetic susceptibility is calculated from the ESR intensity which is considered to be proportional to the product $(A+B)(\Delta H)^2$, where ΔH is the linewidth, after the correction for the skin depth. In Fig. 5, two kinds of corrections are made to estimate the susceptibility. One is associated with the skin depth δ_a parallel to the a axis, where the observed ESR intensity comes from the spins within the skin depth at the surface parallel to the c axis, while the other is ascribed to δ_c parallel to the c axis, where the observed intensity is caused by the spins at the surface parallel to the a axis. The actual situation for the correction stands close to the former though a small part of the contribution to the ESR intensity is attributed to the spins at the surface parallel to the a axis, since the ratio of the observed regions between the two surface sides γ is small, as mentioned in the previous section. Therefore, judging from Fig. 5, the magnetic susceptibility is considered to have a temperature dependence over the whole temperature region, even though the estimation of the ESR intensity includes some ambiguity because of the roughness in the calculation related to the product $(A+B)(\Delta H)^2$. At high temperatures above about 100 K, the susceptibility seems to increase weakly with lowering temperature, while below that temperature, it shows a decrease. The temperature dependence of the susceptibility cannot be explained only with the contribution from the conduction electrons for which the susceptibility obeys a temperature-independent Pauli paramagnetism. The g value is also temperature dependent as shown in Fig. 5. It decreases in the high-temperature region above about 100 K as the temperature is lowered, while it increases below about 100 K. Figure 5 suggests that the temperature dependence of the g value is connected with that of the paramagnetic susceptibility. In the bottlenecked system with the coexistence of conduction-electron spins and localized electron spins such as a dilute alloy CuMn, the g value is described in terms of the magnetic susceptibilities of the conduction-electron spins χ_p and the localized electron spins χ_l, as shown in the following equation:[20]

$$g=\frac{\chi_p g_p+\chi_l g_l}{\chi_p+\chi_l}\ , \tag{4}$$

where g_p and g_l are the g values of the conduction-electron spins and the localized electron spins, respectively, and Eq. (4) is valid only in the low-concentration limit of localized spins. Therefore, the temperature dependences of the magnetic susceptibility and the g value, which are closely correlated with each other as shown here, are thought to be explained by the presence of localized spins in the KH-GIC system, in agreement with the behavior of the diffusion time observed with the ESR measurement. It is very difficult to estimate the concentration of the localized spins because of a considerably large ambiguity, but a rough estimate suggests the concentration of $\sim 10^{-4}$ per K atom, taking into account the magnitude of the temperature dependence of the susceptibility and the electron density of states at the Fermi level $N(E_F)\sim 0.1$ states/eV (C atom) for the Pauli paramagnetism.[6]

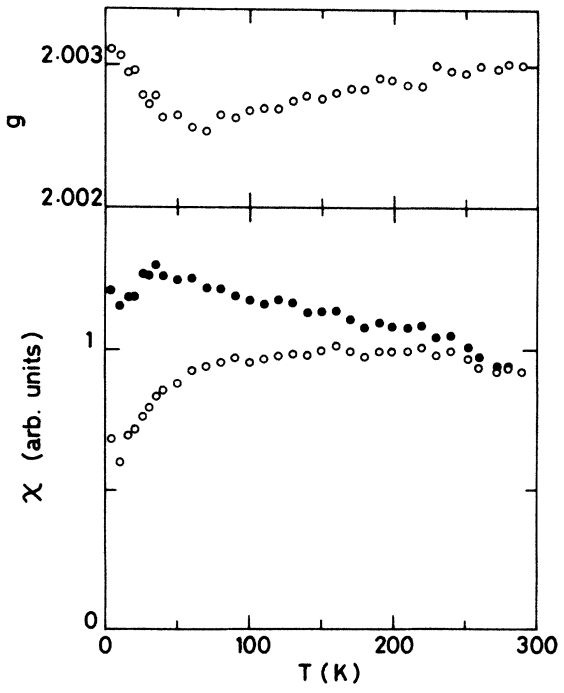

FIG. 5. Temperature dependences of the spin paramagnetic susceptibility χ and the g value for the stage-1 KH-GIC. The open and solid circles denote the susceptibilities after the correction of the ESR intensity for the skin depths parallel to the a and c axes (δ_a and δ_c), respectively.

Next, we discuss the spin relaxation in the KH-GIC system. The temperature dependence of the linewidth ΔH is shown for the stage-1 and -2 KH-GIC's in Fig. 6. At room temperature, we have $\Delta H_\perp=9.5$ G and $\Delta H_\parallel=9.2$ G for the applied fields perpendicular and parallel to the c axis, respectively, for the stage-1 KH-GIC. ΔH decreases linearly in the high-temperature region above about 100 K as the temperature is lowered, while below 100 K it increases steeply and then tends to be constant below about 20 K. The anisotropy in ΔH is temperature dependent and reverses at about 30 K. In the case of the stage-2 KH-GIC, ΔH is smaller than that of the stage-1 KH-GIC; $\Delta H_\perp=2.8$ G and $\Delta H_\parallel=3.2$ G at room temperature. The anisotropy in ΔH at room temperature is opposite to that for the stage-1 KH-GIC, except in the low-temperature region below about 30 K. ΔH shows a weak decrease with lowering temperature in the high-temperature region above about 90 K, but increases steeply below about 80 K. ΔH tends to be constant below about 10 K, reminiscent of the situation in the stage-1 KH-GIC.

Here, we explain the spin relaxation in terms of the contributions from the conduction-electron spins and the localized electron spins. If T_2 is assumed to be caused by the spin-lattice relaxation, the linewidth ΔH can be expressed by the following equation:

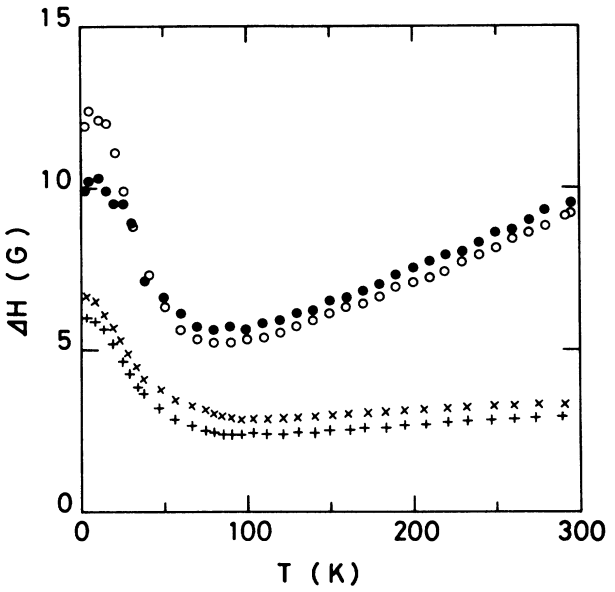

FIG. 6. Temperature dependence of the linewidths ΔH. The stage-1 KH-GIC: ○, H∥c; ●, H⊥c, and the stage-2 KH-GIC: ×, H∥c; +, H⊥c.

$$\Delta H \propto \frac{1}{\chi_p+\chi_l}\left[\frac{\chi_l}{T_l}+\frac{\chi_p}{T_p}\right]. \tag{5}$$

The first term denotes the relaxation process T_l from the localized spins to the lattice, and this contribution is proportional to the susceptibility χ_l due to the localized spins.[20] The second term is associated with the relaxation process T_p from the conduction-electron spins to the lattice, and this contribution is proportional to the Pauli paramagnetic susceptibility χ_p. For the relaxation process with the Elliott mechanism[21] at high temperatures ($T \gg \Theta_D$), T_p is described in the following way:

$$\frac{1}{T_p} \sim \frac{(\Delta g)^2}{\tau_R}, \tag{6}$$

where τ_R is the relaxation time for carrier conduction. The Elliott mechanism plays an important role for the relaxation process related to the conduction electrons in the high-temperature region. The contribution from the Elliott mechanism can be estimated in the following.

In the case of stage-1 KH-GIC, the number of carriers is estimated at $n=2.24\times10^{21}$ cm^{-3}, taking into account the formula unit $C_8K_2H_{2x}$ ($x\sim0.8$). The relaxation time is related to the effective mass of carriers m^* and conductivity σ through the formula $\sigma=ne^2\tau_R/m^*$. Therefore, if we take $m^*=0.2m$ from the Shubnikov–de Haas experiment[7] and $\sigma_a=2.1\times10^4\ \Omega\,\mathrm{cm}^{-1}$ at 300 K,[8] the contribution to the linewidth from the Elliott mechanism, which is expressed by Eq. (6), is found to be ~10 G at 300 K, taking into account the observed g shift $\Delta g_{\parallel}\sim8\times10^{-4}$. The estimated contribution is found to be the same order as the magnitude of the observed linewidth $\Delta H\sim9$ G at 300 K. Since, from Eq. (6), the linewidth related to the Elliott mechanism is proportional to the resistivity at high temperatures, the decrease in the linewidth shown in Fig. 6 is also consistent with the behavior of the linewidth for the Elliott mechanism. Therefore, we can consider that the Elliott mechanism serves mainly for the spin-relaxation process at high temperatures. Sugihara suggests that the linewidth is expected to be 10^{-1} to 10^{-2} G in the Elliott mechanism with graphitic π electrons, which is two or three orders of magnitude smaller than the observed linewidth for alkali GIC's ever known.[22] In order to explain this discrepancy, he proposed a relaxation mechanism where the spin energy in the graphitic π-electron system was relaxed to the lattice system through exchange interactions between the graphitic π and alkali-metal s electrons and the large spin-orbit interaction in alkali-metal atoms. Also in the KH-GIC's, the participation of the K4s electrons might be required to explain the magnitude of the observed linewidth, although the K4s electrons contribute less to the carrier transport in the KH-GIC's than in the alkali-metal binary GIC's.[6,7]

At low temperatures the localized spins contribute to Eq. (5) more than at high temperatures as mentioned for the behaviors of the diffusion time, magnetic susceptibility, and the g value. An increase in the linewidth at low temperature is considered to be associated with the spin-relaxation process with the localized electron spins. To understand the behavior of the linewidth at low temperatures, the surface scattering of the conduction electrons also has to be taken into consideration. GIC's are usually sensitive to air so that the surface irregularity is larger than that in ordinary metals. Therefore, the surface scattering of the conduction electrons is enhanced when lowering the temperature, since the skin depth becomes more shallow at low temperatures. The surface scattering process can contribute partly to the increased linewidth at low temperatures, in addition to the processes mentioned in Eq. (5).

Finally, we will discuss the origin of the localized spins in the present ESR experiment. The presence of localized spins has been reported in several cases of graphite and graphite intercalation compounds. Neutron irradiation[23] and ion implantation with boron[24] generate defects on graphite layers to give localized spins, since these processes are so strong that the network of the bonding between carbon atoms is easily destroyed. The intercalation process was reported to generate localized electrons in alkali-metal graphite intercalation compounds where the ESR signal associated with the localized spins did not show a Dysonian line shape and was not fused with the Dysonian signal due to conduction electrons.[25] Powdered graphite also gives localized spins which are attributed to surface irregularity caused by dangling bonds. The present case with localized spins does not seem to correspond to the conditions in the above cases, since the intercalation process is rather mild, and the observed signal is a fused Dysonian signal. Moreover, the host material is HOPG which *does not possess observable localized spins.* We attempt to explain the present case in the following way.

For the KH-GIC, specific-heat[6] and Shubnikov–de Haas experiments[7] suggest the presence of an ionic lattice

of the donor intercalant with sandwich layers K^+-H^--K^+, which is affected by the conduction electrons on the graphite layers. Therefore, the K^+-H^--K^+ intercalant lattice has similar characteristics to those of pristine alkali-metal hydride K^+-H^-, though the H-NMR experiment[9] suggests the presence of a small concentration of carriers on the hydrogen species in the intercalant lattice, which is 2 orders of magnitude smaller than that of hydrogen atoms of transition-metal hydrides such as PdH_x where the system is regarded as an alloy between Pd and H atoms. The compositions of the KH-GIC's are $C_4KH_{0.8}$ and $C_8KH_{0.8}$ for the stage-1 and -2 compounds, respectively, which suggest a hydrogen deficiency of the ionic intercalant lattice K^+-H^-. The observed localized spins are thought to be caused by the trapped electrons at the defects due to the hydrogen deficiency in the ionic intercalant lattice with a very small concentration of conduction carriers.

The temperature dependences of the diffusion time, the g value, and the paramagnetic susceptibility suggest that the contribution from the localized spins increases as the temperature is lowered. However, the contribution seems to decrease in the low-temperature region below 80–100 K. The surface area within the skin depth where the spins are observed by the ESR measurement is reduced when lowering the temperature, since the skin depth becomes shallow at low temperatures. The hydrogen concentration just beneath the surface is lower than that in the bulk of the sample, since some desorption of hydrogen takes place. The reduction of the hydrogen concentration makes the intercalant lattice near the surface more metallic than that of the bulk, leading to a similar situation to that in the K-GIC's. The metallic features are not favorable for stabilizing the trapped electrons with localized spins in the intercalant lattice. The decrease in the contribution from the localized spins at low temperatures below 80–100 K is considered to be associated with the metallic characters of the intercalant in the near surface area.

IV. SUMMARY

The electronic properties of the stage-1 and -2 KH-GIC's were investigated by means of the ESR measurement in the temperature range between liquid-helium and room temperatures. The ESR spectra show Dysonian line shapes associated with the metallic properties of the KH-GIC's. The experimental results were analyzed by means of the Feher-Kip procedure. This procedure does not give a quantitative analysis for the graphite intercalation compounds which are anisotropic conductors with two dimensionality, and, at the present time, there is no other theoretical treatment for the ESR spectra of the anisotropic conductors. Therefore, we have to be satisfied with rather qualitative explanations of the experimental results in this paper.

The diffusion time T_D estimated with the asymmetry parameter A/B of the Dysonian signal is found to be larger than the diffusion time obtained from conductivity measurement. This suggests the presence of localized spins interacting with conduction-electron spins. The g value and the paramagnetic susceptibility possess temperature dependences. The temperature dependence of the g value is well correlated with that of the susceptibility. This finding is reminiscent of the behaviors in a dilute alloy CuMn, which is regarded at the bottlenecked system with the coexistence of conduction-electron spins and localized electron spins. Therefore, the ESR signals of the KH-GIC's are associated not only with conduction-electron spins but also with localized electron spins. The KH-GIC's possess the ionic lattice of the donor intercalant with sandwich triple layers K^+-H^--K^+, which is affected by the conduction electrons on graphite layers. The composition of $C_{4n}KH_{0.8}$ suggests a hydrogen deficiency in the K^+-H^--K^+ ionic intercalant, which gives defects in the intercalant. The presence of the localized spins is attributed to trapped electrons at the defects in the intercalant.

The linewidth ΔH decreases linearly as the temperature is lowered in the high-temperature range. As well as the temperature dependence of ΔH, the magnitude of ΔH can be explained with the Elliott mechanism of the spin relaxation for conduction electrons at high temperatures. Judging from the magnitude of ΔH, the spin energy in conduction electrons which stay mainly on the graphite band is relaxed to the lattice system through exchange interactions between graphite π and alkali-metal s electrons and the large spin-orbit interaction in alkali-metal atoms. At low temperatures, ΔH is enhanced with the lowering of temperature. The increase in ΔH is considered to be associated with the spin-relaxation process with localized electron spins. The surface scattering process can also contribute to the increase in ΔH at low temperatures as well as the process with localized spins.

ACKNOWLEDGMENTS

The authors thank Dr. A. W. Moore of Union Carbide for his generous gift of HOPG. They also would like to express their gratitude to Dr. K. Sugihara, Professor M. S. Dresselhaus, Dr. G. Dresselhaus, and Professor S. Sako for valuable discussions. This work was supported by the Grant-in-Aid for Scientific Research No. 61540250 from the Ministry of Education, Science and Culture, Japan.

*Present address: Department of Chemistry, Faculty of Science, Tokyo Institute of Technology, Ookayama, Meguro-ku, Tokyo 152, Japan.

[1]H. Inokuchi, N. Wakayama, T. Kondow, and Y. Mori, J. Chem. Phys. **46**, 837 (1967).

[2]M. Colin and A. Hérold, Bull. Soc. Chim. Fr. **1971**, 1982 (1971).

[3]G. Furdin, P. Lagrange, A. Hérold, and C. Zeller, C. R. Acad. Soc. Ser. C **282**, 563 (1976).

[4]D. Guérard, C. Takoudjou, and F. Rousseaux, Synth. Metals **7**, 43 (1983).

[5]L. Salamanmca-Riba, N.-C. Yeh, M. S. Dresselhaus, M. Endo,

and T. Enoki, J. Mater. Res. **1**, 177 (1986).
[6]T. Enoki, M. Sano, and H. Inokuchi, Phys. Rev. B **32**, 2497 (1985).
[7]T. Enoki, N.-C. Yeh, S.-T. Chen, and M. S. Dresselhaus, Phys. Rev. B **33**, 1292 (1986).
[8]T. Enoki, K. Imaeda, H. Inokuchi, and M. Sano, Phys. Rev. B **35**, 9399 (1987).
[9]S. Miyajima, T. Chiba, T. Enoki, H. Inokuchi, and M. Sano Phys. Rev. B **37**, 3246 (1988).
[10]K. A. Müller and R. Kleiner, Phys. Lett. **1**, 98 (1962).
[11]S. K. Khanna, E. R. Falardeau, A. J. Heeger, and J. E. Fischer, Solid State Commun. **25**, 1059 (1978).
[12]P. Lauginie, H. Estrade, J. Conard, D. Guérard, P. Lagrange, and M. El Markrini, Physica **99B**, 514 (1980).
[13]M. Murata and H. Suematsu, J. Phys. Soc. Jpn. **51**, 1337 (1982).
[14]P. Delhaes, J. Amiell, K. Ohhashi, J. F. Mareché, D. Guérard, and A. Hérold, Synth. Metals **8**, 269 (1983).
[15]D. Davidov, O. Milo, I. Palchan, and H. Selig, Synth. Metals **10**, 101 (1984).
[16]R. M. Stein, L. Walmsley, and C. Rettori, Phys. Rev. B **32**, 4134 (1985).
[17]J. Blinowski, P. Kacman, C. Rigaux, and M. Saint-Jean, Synth. Metals **12**, 419 (1985).
[18]M. Saint-Jean, C. Rigaux, B. Clerjaud, J. Blinowski, P. Kacman, and G. Furdin, J. Phys. (Paris) (to be published).
[19]G. Feher and A. F. Kip, Phys. Rev. **98**, 337 (1955).
[20]S. Schultz, M. R. Shanabarger, and P. M. Platzman, Phys. Rev. Lett. **19**, 749 (1967).
[21]R. J. Elliott, Phys. Rev. **96**, 266 (1954).
[22]K. Sugihara, J. Phys. Soc. Jpn. **53**, 393 (1984).
[23]K. A. Müller, Phys. Rev. **123**, 1550 (1961).
[24]K. Kawamura, S. Kaneko, and T. Tsuzuku, J. Phys. Soc. Jpn. **52**, 3936 (1983).
[25]M. Murata, M. Sc. thesis, University of Tsukuba, 1982 (unpublished).